USGS
science for a changing world

Techniques of Water-Resources Investigations
of the United States Geological Survey

Chapter C2

COMPUTER MODEL OF TWO-DIMENSIONAL SOLUTE TRANSPORT AND DISPERSION IN GROUND WATER

By L. F. Konikow and J. D. Bredehoeft

Book 7

AUTOMATED DATA PROCESSING AND COMPUTATIONS

DEPARTMENT OF THE INTERIOR

WILLIAM P. CLARK, Secretary

U.S. GEOLOGICAL SURVEY

Dallas L. Peck, Director

Requests, at cost, for the Card Deck listed in Attachment VII should be directed to:
Ralph N. Eicher, Chief, Office of Teleprocessing, M.S. 805, National Center,
U.S. Geological Survey, Reston, Virginia 22092.

First printing 1978
Second printing 1984

UNITED STATES GOVERNMENT PRINTING OFFICE, WASHINGTON : **1978**

For sale by the Distribution Branch, U.S. Geological Survey
604 South Pickett Street, Alexandria, VA 22304

PREFACE

The series of manuals on techniques describes procedures for planning and executing specialized work in water-resources investigations. The material is grouped under major headings called books and further subdivided into sections and chapters; section C of Book 7 is on computer programs.

This chapter presents a digital computer model for calculating changes in the concentration of a dissolved chemical species in flowing ground water. The computer program represents a basic and general model that may have to be modified by the user for efficient application to his specific field problem. Although this model will produce reliable calculations for a wide variety of field problems, the user is cautioned that in some cases the accuracy and efficiency of the model can be affected significantly by his selection of values for certain user-specified options.

CONTENTS

FIGURES

FIGURES—Continued

TABLES

COMPUTER MODEL OF TWO-DIMENSIONAL SOLUTE TRANSPORT AND DISPERSION IN GROUND WATER

By L. F. Konikow and J. D. Bredehoeft

Abstract

This report presents a model that simulates solute transport in flowing ground water. The model is both general and flexible in that it can be applied to a wide range of problem types. It is applicable to one- or two-dimensional problems involving steady-state or transient flow. The model computes changes in concentration over time caused by the processes of convective transport, hydrodynamic dispersion, and mixing (or dilution) from fluid sources. The model assumes that the solute is nonreactive and that gradients of fluid density, viscosity, and temperature do not affect the velocity distribution. However, the aquifer may be heterogeneous and (or) anisotropic.

The model couples the ground-water flow equation with the solute-transport equation. The digital computer program uses an alternating-direction implicit procedure to solve a finite-difference approximation to the ground-water flow equation, and it uses the method of characteristics to solve the solute-transport equation. The latter uses a particle-tracking procedure to represent convective transport and a two-step explicit procedure to solve a finite-difference equation that describes the effects of hydrodynamic dispersion, fluid sources and sinks, and divergence of velocity. This explicit procedure has several stability criteria, but the consequent time-step limitations are automatically determined by the program.

The report includes a listing of the computer program, which is written in FORTRAN IV and contains about 2,000 lines. The model is based on a rectangular, block-centered, finite-difference grid. It allows the specification of any number of injection or withdrawal wells and of spatially varying diffuse recharge or discharge, saturated thickness, transmissivity, boundary conditions, and initial heads and concentrations. The program also permits the designation of up to five nodes as observation points, for which a summary table of head and concentration versus time is printed at the end of the calculations. The data input formats for the model require three data cards and from seven to nine data sets to describe the aquifer properties, boundaries, and stresses.

The accuracy of the model was evaluated for two idealized problems for which analytical solutions could be obtained. In the case of one-dimensional flow the agreement was nearly exact, but in the case of plane radial flow a small amount of numerical dispersion occurred. An analysis of several test problems indicates that the error in the mass balance will be generally less than 10 percent. The test problems demonstrated that the accuracy and precision of the numerical solution is sensitive to the initial number of particles placed in each cell and to the size of the time increment, as determined by the stability criteria. Mass balance errors are commonly the greatest during the first several time increments, but tend to decrease and stabilize with time.

Introduction

This report describes and documents a computer model for calculating transient changes in the concentration of a nonreactive solute in flowing ground water. The computer program solves two simultaneous partial differential equations. One equation is the ground-water flow equation, which describes the head distribution in the aquifer. The second is the solute-transport equation, which describes the chemical concentration in the system. By coupling the flow equation with the solute-transport equation, the model can be applied to both steady-state and transient flow problems.

The purpose of the simulation model is to compute the concentration of a dissolved chemical species in an aquifer at any specified place and time. Changes in chemical concentration occur within a dynamic ground-water system primarily due to four

distinct processes: (1) convective transport, in which dissolved chemicals are moving with the flowing ground water; (2) hydrodynamic dispersion, in which molecular and ionic diffusion and small-scale variations in the velocity of flow through the porous media cause the paths of dissolved molecules and ions to diverge or spread from the average direction of ground-water flow; (3) fluid sources, where water of one composition is introduced into water of a different composition; and (4) reactions, in which some amount of a particular dissolved chemical species may be added to or removed from the ground water due to chemical and physical reactions in the water or between the water and the solid aquifer materials. The model presented in this report assumes (1) that no reactions occur that affect the concentration of the species of interest, and (2) that gradients of fluid density, viscosity, and temperature do not affect the velocity distribution.

This model can be applied to a wide variety of field problems. However, the user should first become aware of the assumptions and limitations inherent in the model, as described in this report. The computer program presented in this report is offered as a basic working tool that may have to be modified by the user for efficient application to specific field problems. The program is written in FORTRAN IV and is compatible with most high-speed computers. The data requirements, input format specifications, program options, and output formats are all structured in a general manner that should be readily adaptable to many field problems.

This report includes a detailed description of the numerical method used to solve the solute-transport equation. The reader is assumed to have (or can obtain elsewhere) a moderate familiarity with finite-difference methods and ground-water flow models.

Theoretical Background

Flow equation

By following the derivation of Pinder and Bredehoeft (1968), the equation describing the transient two-dimensional areal flow of a homogeneous compressible fluid through a nonhomogeneous anisotropic aquifer can be written in Cartesian tensor notation as

$$\frac{\partial}{\partial x_i}\left(T_{ij}\frac{\partial h}{\partial x_j}\right) = S\frac{\partial h}{\partial t} + W \qquad i,j = 1,2 \qquad (1)$$

where

T_{ij} is the transmissivity tensor, L^2/T;
h is the hydraulic head, L;
S is the storage coefficient, (dimensionless);
t is the time, T;
$W = W(x,y,t)$ is the volume flux per unit area (positive sign for outflow and negative for inflow), L/T; and
x_i and x_j are the Cartesian coordinates, L.

If we only consider fluxes of (1) direct withdrawal or recharge, such as well pumpage, well injection, or evapotranspiration, and (2) steady leakage into or out of the aquifer through a confining layer, streambed, or lakebed, then $W(x,y,t)$ may be expressed as

$$W(x,y,t) = Q(x,y,t) - \frac{K_z}{m}(H_s - h) \qquad (2)$$

where

Q is the rate of withdrawal (positive sign) or recharge (negative sign), L/T;
K_z is the vertical hydraulic conductivity of the confining layer, streambed, or lakebed, L/T;
m is the thickness of the confining layer, streambed, or lakebed, L; and
H_s is the hydraulic head in the source bed, stream, or lake, L.

Lohman (1972) shows that an expression for the average seepage velocity of ground water can be derived from Darcy's law. This expression can be written in Cartesian tensor notation as

$$V_i = -\frac{K_{ij}}{\epsilon}\frac{\partial h}{\partial x_j} \qquad (3)$$

where

V_i is the seepage velocity in the direction of x_i, L/T;
K_{ij} is the hydraulic conductivity tensor, L/T; and
ϵ is the effective porosity of the aquifer, (dimensionless).

Transport equation

The equation used to describe the two-dimensional areal transport and dispersion of a given nonreactive dissolved chemical species in flowing ground water was derived by Reddell and Sunada (1970), Bear (1972), Bredehoeft and Pinder (1973), and Konikow and Grove (1977). The equation may be written as

$$\frac{\partial(Cb)}{\partial t}=\frac{\partial}{\partial x_i}\left(bD_{ij}\frac{\partial C}{\partial x_j}\right)-\frac{\partial}{\partial x_i}(bCV_i)-\frac{C'W}{\epsilon} \qquad i,j=1,2 \quad (4)$$

where

C is the concentration of the dissolved chemical species, M/L^3;
D_{ij} is the coefficient of hydrodynamic dispersion (a second-order tensor), L^2/T;
b is the saturated thickness of the aquifer, L; and
C' is the concentration of the dissolved chemical in a source or sink fluid, M/L^3.

The first term on the right side of equation 4 represents the change in concentration due to hydrodynamic dispersion. The second term describes the effects of convective transport, while the third term represents a fluid source or sink.

Dispersion coefficient

Bear (1972, p. 580–581) states that hydrodynamic dispersion is the macroscopic outcome of the actual movements of individual tracer particles through the pores and that it includes two processes. One process is mechanical dispersion, which depends upon both the flow of the fluid and the nature of the pore system through which the flow takes place. The second process is molecular and ionic diffusion, which because it depends on time, is more significant at low flow velocities. Bear (1972) further states that the separation between the two processes is artificial. In developing our model we assume for flowing ground-water systems that the definable contribution of molecular and ionic diffusion to hydrodynamic dispersion is negligible.

The dispersion coefficient may be related to the velocity of ground-water flow and to the nature of the aquifer using Scheidegger's (1961) equation:

$$D_{ij}=\alpha_{ijmn}\frac{V_mV_n}{|V|} \qquad (5)$$

where

α_{ijmn} is the dispersivity of the aquifer, L;
V_m and V_n are components of velocity in the m and n directions, respectively, L/T; and
$|V|$ is the magnitude of the velocity, L/T.

Scheidegger (1961) further shows that for an isotropic aquifer the dispersivity tensor can be defined in terms of two constants. These are the longitudinal and transverse dispersivities of the aquifer (α_L and α_T, respectively). These are related to the longitudinal and transverse dispersion coefficients by

$$D_L=\alpha_L|V| \qquad (6)$$

and

$$D_T=\alpha_T|V|. \qquad (7)$$

After expanding equation 5, substituting Scheidegger's identities, and eliminating terms with coefficients that equal zero, the components of the dispersion coefficient for two-dimensional flow in an isotropic aquifer may be stated explicitly as

$$D_{xx}=D_L\frac{(V_x)^2}{|V|^2}+D_T\frac{(V_y)^2}{|V|^2}; \qquad (8)$$

$$D_{yy}=D_T\frac{(V_x)^2}{|V|^2}+D_L\frac{(V_y)^2}{|V|^2}; \qquad (9)$$

$$D_{xy}=D_{yx}=(D_L-D_T)\frac{V_xV_y}{|V|^2}. \qquad (10)$$

Note that while D_{xx} and D_{yy} must have positive values, it is possible for the cross-product terms (eq 10) to have negative values if V_x and V_y have opposite signs.

Review of assumptions

A number of assumptions have been made in the development of the previous equations. Following is a list of the main assumptions that must be carefully evaluated before applying the model to a field problem.

1. Darcy's law is valid and hydraulic-head gradients are the only significant driving mechanism for fluid flow.
2. The porosity and hydraulic conductivity of the aquifer are constant with time, and porosity is uniform in space.
3. Gradients of fluid density, viscosity, and temperature do not affect the velocity distribution.
4. No chemical reactions occur that affect the concentration of the solute, the fluid properties, or the aquifer properties.
5. Ionic and molecular diffusion are negligible contributors to the total dispersive flux.
6. Vertical variations in head and concentration are negligible.
7. The aquifer is homogeneous and isotropic with respect to the coefficients of longitudinal and transverse dispersivity.

The nature of a specific field problem may be such that not all of these underlying assumptions are completely valid. The degree to which field conditions deviate from these assumptions will affect the applicability and reliability of the model for that problem. If the deviation from a particular assumption is significant, the governing equations will have to be modified to account for the appropriate processes or factors.

Numerical Methods

Because aquifers have variable properties and complex boundary conditions, exact analytical solutions to the partial differential equations of flow (eq 1) and solute transport (eq 4) cannot be obtained directly. Therefore, approximate numerical methods must be employed.

The numerical methods require that the area of interest be subdivided by a grid into a number of smaller subareas. The model developed here utilizes a rectangular, uniformly spaced, block-centered, finite-difference grid, in which nodes are defined at the centers of the rectangular cells.

Flow equation

Pinder and Bredehoeft (1968) show that if the coordinate axes are alined with the principal directions of the transmissivity tensor, equation 1 may be approximated by the following implicit finite-difference equation:

$$\begin{aligned}
&T_{xx[i-\frac{1}{2},j]}\left[\frac{h_{i-1,j,k}-h_{i,j,k}}{(\Delta x)^2}\right]\\
&\quad+T_{xx[i+\frac{1}{2},j]}\left[\frac{h_{i+1,j,k}-h_{i,j,k}}{(\Delta x)^2}\right]\\
&\quad+T_{yy[i,j-\frac{1}{2}]}\left[\frac{h_{i,j-1,k}-h_{i,j,k}}{(\Delta y)^2}\right]\\
&\quad+T_{yy[i,j+\frac{1}{2}]}\left[\frac{h_{i,j+1,k}-h_{i,j,k}}{(\Delta y)^2}\right]\\
&=S\left[\frac{h_{i,j,k}-h_{i,j,k-1}}{\Delta t}\right]\\
&\quad+\frac{q_{w(i,j)}}{\Delta x\Delta y}\quad\frac{K_z}{m}[H_{s(i,j)}-h_{i,j,k}] \qquad (11)
\end{aligned}$$

where

i,j,k are indices in the x, y, and time dimensions, respectively;

$\Delta x,\Delta y,\Delta t$ are increments in the x, y, and time dimensions, respectively; and

q_w is the volumetric rate of withdrawal or recharge at the (i,j) node, L^3/T.

Note that k represents the new time level and k–1 represents the previous time level. To avoid confusion between tensor sub-

scripts and nodal indices, the latter are separated by commas.

The finite-difference equation (eq 11) is solved numerically for each node in the grid using an iterative alternating-direction implicit (ADI) procedure. The derivation and solution of the finite-difference equation and the use of the iterative ADI procedure have been previously discussed in detail in the literature. Some of the more relevant references include Pinder and Bredehoeft (1968), Prickett and Lonnquist (1971), and Trescott, Pinder, and Larson (1976).

After the head distribution has been computed for a given time step, the velocity of ground-water flow is computed at each node using an explicit finite-difference form of equation 3. For example, the velocity in the x direction at node (i,j) would be computed as

$$V_{x(i,j)} = \frac{K_{xx(i,j)}}{\epsilon} \frac{(h_{i-1,j,k} - h_{i+1,j,k})}{2\Delta x}. \quad (12)$$

The velocity in the x direction can also be computed on the boundary between node (i,j) and node $(i+1,j)$ using the following equation:

$$V_{x(i+\frac{1}{2},j)} = \frac{K_{xx(i+\frac{1}{2},j)}}{\epsilon} \frac{(h_{i,j,k} - h_{i+1,j,k})}{\Delta x} \quad (13)$$

where the hydraulic conductivity on the boundary is computed as the harmonic mean of the hydraulic conductivities at the two adjacent nodes.

Expressions similar to equations 12 and 13 are used to compute the velocities in the y direction at (i,j) and $(i,j+\frac{1}{2})$ respectively. Note that equation 13, which computes the head difference over a distance Δx, is more accurate than equation 12, which computes the head difference over $2\Delta x$.

Transport equation

Method of characteristics

The method of characteristics is used in this model to solve the solute-transport equation. This method was developed to solve hyperbolic differential equations. If solute transport is dominated by convective transport, as is common in many field problems, then equation 4 may closely approximate a hyperbolic partial differential equation and be highly compatible with the method of characteristics. Although it is difficult to present a rigorous mathematical proof for this numerical scheme, it has been successfully applied to a variety of field problems. The development of this technique for problems of flow through porous media has been presented by Garder, Peaceman, and Pozzi (1964), Pinder and Cooper (1970), Reddell and Sunada (1970), and Bredehoeft and Pinder (1973). Garder, Peaceman, and Pozzi (1964) state that this technique does not introduce numerical dispersion (artificial dispersion resulting from the numerical calculation process). They and Reddell and Sunada (1970) also compared solutions obtained using the method of characteristics with those derived by analytical methods and found good agreement for the cases investigated. Applications of the method to field problems have been documented by Bredehoeft and Pinder (1973), Konikow and Bredehoeft (1974), Robertson (1974), Robson (1974), and Konikow (1977).

The approach taken by the method of characteristics is not to solve equation 4 directly, but rather to solve an equivalent system of ordinary differential equations. Konikow and Grove (1977, eq 61) show that by considering saturated thickness as a variable and by expanding the convective transport term, equation 4 may be rewritten as

$$\frac{\partial C}{\partial t} = \frac{1}{b}\frac{\partial}{\partial x_i}\left(bD_{ij}\frac{\partial C}{\partial x_j}\right) - V_i\frac{\partial C}{\partial x_i} + \frac{C\left(S\frac{\partial h}{\partial t} + W - \epsilon\frac{\partial b}{\partial t}\right) - C'W}{\epsilon b}. \quad (14)$$

Equation 14 is the form of the solute-transport equation that is solved in the computer program presented in this report. For convenience we may also write equation 14 as

$$\frac{\partial C}{\partial t} = \frac{1}{b}\frac{\partial}{\partial x_i}\left(bD_{ij}\frac{\partial C}{\partial x_j}\right) - V_x\frac{\partial C}{\partial x} - V_y\frac{\partial C}{\partial y} + F \quad (15)$$

where

$$F=\frac{C(S\frac{\partial h}{\partial t}+W-\epsilon\frac{\partial b}{\partial t})-C'W}{\epsilon b}. \quad (16)$$

Next consider representative fluid particles that are convected with flowing ground water. Note that changes with time in properties of the fluid, such as concentration, may be described either for fixed points within a stationary coordinate system as successive fluid particles pass the reference points, or for reference fluid particles as they move along their respective paths past fixed points in space. Aris (1962, p. 78) states that "associated with these two descriptions are two derivatives with respect to time." Thus $\partial C/\partial t$ is the rate of change of concentration as observed from a fixed point, whereas dC/dt is the rate of change as observed when moving with the fluid particle. Aris (1962) calls the latter the *material derivative.*

The material derivative of concentration may be defined as

$$\frac{dC}{dt}=\frac{\partial C}{\partial t}+\frac{\partial C}{\partial x}\frac{dx}{dt}+\frac{\partial C}{\partial y}\frac{dy}{dt}. \quad (17)$$

Note the correspondence of the second and third terms on the right side of equation 15 with the second and third terms on the right side of equation 17. The latter includes the material derivatives of position, which are defined by velocity. Thus for the x and y components, respectively, of position and velocity we have

$$\frac{dx}{dt}=V_x \quad (18)$$

and

$$\frac{dy}{dt}=V_y. \quad (19)$$

If we next substitute the right sides of equations 15, 18, and 19 for the corresponding terms in equation 17, we obtain

$$\frac{dC}{dt}=\frac{1}{b}\frac{\partial}{\partial x_i}(bD_{ij}\frac{\partial C}{\partial x_j})+F. \quad (20)$$

The solutions of the system of equations comprising equations 18–20 may be given as

$$x=x(t)\,;\ y=y(t)\,;\ \text{and}\ C=C(t) \quad (21)$$

and are called the characteristic curves of equation 15.

Given solutions to equations 18–20, a solution to the partial differential equation (eq 15) may be obtained by following the characteristic curves. This is accomplished numerically by introducing a set of moving points (or reference particles) that can be traced within the stationary coordinates of the finite-difference grid. Garder, Peaceman, and Pozzi (1964, p. 27) state, "Each point corresponds to one characteristic curve, and values of x, y, and C are obtained as functions of t for each characteristic." Each point has a concentration and position associated with it and is moved through the flow field in proportion to the flow velocity at its location. Intuitively, the method may be visualized as tracing a number of fluid particles through a flow field and observing changes in chemical concentration in the fluid particles as they move.

Particle tracking

The first step in the method of characteristics involves placing a number of traceable particles or points in each cell of the finite-difference grid to form a set of points that are distributed in a geometrically uniform pattern throughout the area of interest. It was found that placing from four to nine points per cell provided satisfactory results for most two-dimensional problems. The location or position of each particle is specified by its x- and y- coordinates in the finite-difference grid. The initial concentration assigned to each point is the initial concentration associated with the node of the cell containing the point.

For each time step every point is moved a distance proportional to the length of the time increment and the velocity at the location of the point. (See fig. 1.) The new position of a point is thus computed with the following finite-difference forms of equations 18 and 19:

$$x_{p,k}=x_{p,k-1}+\delta x_p=x_{p,k-1}+\Delta t V_{x[x_{(p,k)},y_{(p,k)}]} \quad (22)$$

and

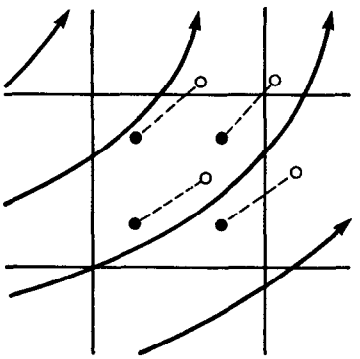

EXPLANATION

- ● Initial location of particle
- O New location of particle
- → Flow line and direction of flow
- --- Computed path of particle

Figure 1.—Part of hypothetical finite-difference grid showing relation of flow field to movement of points.

$$y_{p,k}=y_{p,k-1}+\delta y_p=y_{p,k-1}+\Delta t V_{y[x_{(p,k)},y_{(p,k)}]} \quad (23)$$

where

p is the index number for point identification; and

δx_p and δy_p are the distances moved in the x and y directions, respectively.

The x and y velocities at the position of any particular point p, indicated as $V_{i[x_{(p,k)},y_{(p,k)}]}$, for time k are calculated through bilinear interpolation over the area of half of a cell using the x and y velocities computed at adjacent nodes and cell boundaries. For example, figure 2 illustrates that the velocity in the x direction of point p, located in the southeast quadrant of cell (i,j), would be computed using bilinear interpolation between the x velocities computed with equations 12 and 13 at (i,j), $(i,j+1)$, $(i+\frac{1}{2},j)$, and $(i+\frac{1}{2},j+1)$. Similarly, the velocity in the y direction of point p would be based on the y velocities computed at (i,j), $(i+1,j)$, $(i,j+\frac{1}{2})$ and $(i+1,j+\frac{1}{2})$.

After all points have been moved, the concentration at each node is temporarily assigned the average of the concentrations of all points then located within the area of that cell; this average concentration is denoted as $C_{i,j,k*}$. The time index is distinguished with an asterisk here because this temporarily assigned average concentration represents the new time level only with respect to convective transport. The moving points simulate convective transport because the concentration at each node of the grid will change with each time step as different points having different concentrations enter and leave the area of that cell.

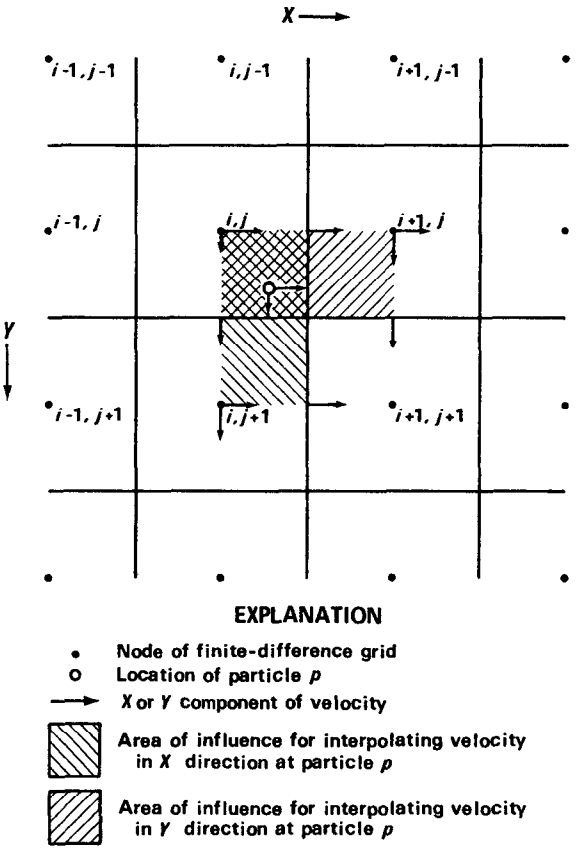

EXPLANATION

- • Node of finite-difference grid
- O Location of particle p
- → X or Y component of velocity
- Area of influence for interpolating velocity in X direction at particle p
- Area of influence for interpolating velocity in Y direction at particle p

Figure 2.—Part of hypothetical finite-difference grid showing areas over which bilinear interpolation is used to compute the velocity at a point. Note that each area of influence is equal to one-half of the area of a cell.

Finite-difference approximations

The total change in concentration in an aquifer may be computed by solving equations 18–20. Equations 18 and 19, which are related to changes in concentration caused

by convective transport alone, are solved by the movement of points as described previously. The changes in concentration caused by hydrodynamic dispersion, fluid sources, divergence of velocity, and changes in saturated thickness are calculated using an explicit finite-difference approximation to equation 20, which can be expressed as

$$\Delta C_{i,j,k}=\Delta t\left[\frac{1}{b}\frac{\partial}{\partial x_i}\left(bD_{ij}\frac{\partial C}{\partial x_j}\right)+F\right]. \quad (24)$$

Note that a solution to equation 20 requires the computation of the change in concentration at the tracer particles. However, primarily because of the difficulty in computing the concentration gradient at a large number of moving points, the change in concentration represented by equation 20 is solved at each node of the grid rather than directly at the location of each point. The material derivative of concentration on any characteristic curve (or for any tracer particle) is then related to the change in concentration for a node during one time step, which was computed with the solution to equation 24.

The right side of equation 24 can be considered as the sum of two separate terms, as follows:

$$\Delta C_{i,j,k}=(\Delta C_{i,j,k})_{\mathrm{I}}+(\Delta C_{i,j,k})_{\mathrm{II}} \quad (25)$$

where

$(\Delta C_{i,j,k})_{\mathrm{I}}$ is the change in concentration caused by hydrodynamic dispersion, and is defined as

$$(\Delta C_{i,j,k})_{\mathrm{I}}=\frac{\Delta t}{b}\left[\frac{\partial}{\partial x_i}\left(bD_{ij}\frac{\partial C}{\partial x_j}\right)\right] \quad (26)$$

and

$(\Delta C_{i,j,k})_{\mathrm{II}}$ is the change in concentration resulting from an external fluid source and changes in saturated thickness, and from equation 16 is defined as

$$(\Delta C_{i,j,k})_{\mathrm{II}}=\Delta t\,F=\Delta t\left[\frac{C\left(S\frac{\partial h}{\partial t}+W-\epsilon\frac{\partial b}{\partial t}\right)-C'W}{\epsilon b}\right]. \quad (27)$$

First we will examine the change in concentration due to dispersion, partly following the development of Reddell and Sunada (1970). The right side of equation 26 can be expanded according to the summation convention of tensor notation to obtain

$$(\Delta C_{i,j,k})_{\mathrm{I}}=\frac{\Delta t}{b}\left[\frac{\partial}{\partial x}\left(bD_{xx}\frac{\partial C}{\partial x}+bD_{xy}\frac{\partial C}{\partial y}\right)+\frac{\partial}{\partial y}\left(bD_{yy}\frac{\partial C}{\partial y}+bD_{yx}\frac{\partial C}{\partial x}\right)\right]. \quad (28)$$

A finite-difference approximation for the derivative in the x direction at (i,j) may be written as

$$\frac{\partial}{\partial x}\left(bD_{xx}\frac{\partial C}{\partial x}+bD_{xy}\frac{\partial C}{\partial y}\right)=\frac{\partial}{\partial x}\left(bD_{xx}\frac{\partial C}{\partial x}\right)+\frac{\partial}{\partial x}\left(bD_{xy}\frac{\partial C}{\partial y}\right)=\frac{\left(bD_{xx}\frac{\partial C}{\partial x}\right)_{i+\frac{1}{2},j}-\left(bD_{xx}\frac{\partial C}{\partial x}\right)_{i-\frac{1}{2},j}}{\Delta x}+\frac{\left(bD_{xy}\frac{\partial C}{\partial y}\right)_{i+\frac{1}{2},j}-\left(bD_{xy}\frac{\partial C}{\partial y}\right)_{i-\frac{1}{2},j}}{\Delta x}. \quad (29)$$

In the following expansion of equation 29 it is implied that concentrations (C) are known from the previous (k–1) time level; hence, equation 29 is an explicit finite-difference equation. The spatial derivatives of concentration at $(i+\frac{1}{2},j)$ may be approximated by

$$\left(\frac{\partial C}{\partial x}\right)_{i+\frac{1}{2},j}=\frac{C_{i+1,j}-C_{i,j}}{\Delta x} \quad (30)$$

and

$$\left(\frac{\partial C}{\partial y}\right)_{i+\frac{1}{2},j}=\frac{C_{i+\frac{1}{2},j+1}-C_{i+\frac{1}{2},j-1}}{2\Delta y}. \quad (31)$$

Because concentrations are defined only at nodes, we must express the right side of equation 31 in terms of concentrations at nodes. Assuming that the concentration at a

cell boundary is approximately equal to the average (arithmetic mean) of the concentrations at adjacent nodes, we have

$$C_{i+\frac{1}{2},j+1} = \frac{C_{i,j+1} + C_{i+1,j+1}}{2} \tag{32}$$

and

$$C_{i+\frac{1}{2},j-1} = \frac{C_{i,j-1} + C_{i+1,j-1}}{2}. \tag{33}$$

Substitution of equations 32 and 33 into equation 31 results in:

$$\left(\frac{\partial C}{\partial y}\right)_{i+\frac{1}{2},j} = \frac{C_{i,j+1} + C_{i+1,j+1} - C_{i,j-1} - C_{i+1,j-1}}{4\Delta y}. \tag{34}$$

Similarly, the spatial derivatives of concentration at $(i-\frac{1}{2},j)$ are

$$\left(\frac{\partial C}{\partial x}\right)_{i-\frac{1}{2},j} = \frac{C_{i,j} - C_{i-1}}{\Delta x} \tag{35}$$

and

$$\left(\frac{\partial C}{\partial y}\right)_{i-\frac{1}{2},j} = \frac{C_{i-1,j+1} + C_{i,j+1} - C_{i-1,j-1} - C_{i,j-1}}{4\Delta y}. \tag{36}$$

After substituting equations 30, 34, 35, and 36 into equation 29, we have

$$\begin{aligned}\frac{\partial}{\partial x}\left(bD_{xx}\frac{\partial C}{\partial x} + bD_{xy}\frac{\partial C}{\partial y}\right) &= \frac{bD_{xx[i+\frac{1}{2},j]}(C_{i+1,j} - C_{i,j})}{(\Delta x)^2} - \frac{bD_{xx[i-\frac{1}{2},j]}(C_{i,j} - C_{i-1,j})}{(\Delta x)^2} \\ &+ \frac{bD_{xy[i+\frac{1}{2},j]}(C_{i,j+1} + C_{i+1,j+1} - C_{i,j-1} - C_{i+1,j-1})}{4\Delta x \Delta y} \\ &- \frac{bD_{xy[i-\frac{1}{2},j]}(C_{i-1,j+1} + C_{i,j+1} - C_{i-1,j-1} - C_{i,j-1})}{4\Delta x \Delta y}.\end{aligned} \tag{37}$$

A finite-difference approximation for the derivative in the y direction in equation 28 may be developed for node (i,j) in an analogous manner to equation 37 to produce

$$\begin{aligned}\frac{\partial}{\partial y}\left(bD_{yy}\frac{\partial C}{\partial y} + bD_{yx}\frac{\partial C}{\partial x}\right) &= \frac{\left(bD_{yy}\frac{\partial C}{\partial y}\right)_{i,j+\frac{1}{2}} - \left(bD_{yy}\frac{\partial C}{\partial y}\right)_{i,j-\frac{1}{2}}}{\Delta y} + \frac{\left(bD_{yx}\frac{\partial C}{\partial x}\right)_{i,j+\frac{1}{2}} - \left(bD_{yx}\frac{\partial C}{\partial x}\right)_{i,j-\frac{1}{2}}}{\Delta y} \\ &= \frac{bD_{yy[i,j+\frac{1}{2}]}(C_{i,j+1} - C_{i,j})}{(\Delta y)^2} - \frac{bD_{yy[i,j-\frac{1}{2}]}(C_{i,j} - C_{i,j-1})}{(\Delta y)^2} \\ &+ \frac{bD_{yx[i,j+\frac{1}{2}]}(C_{i+1,j} + C_{i+1,j+1} - C_{i-1,j} - C_{i-1,j+1})}{4\Delta x \Delta y} \\ &- \frac{bD_{yx[i,j-\frac{1}{2}]}(C_{i+1,j-1} + C_{i+1,j} - C_{i-1,j-1} - C_{i-1,j})}{4\Delta x \Delta y}.\end{aligned} \tag{38}$$

Equation 28 may then be solved explicitly by substituting the relationships expressed by equations 37 and 38 for the terms within brackets on the right side of equation 28.

Next we will examine the change in concentration denoted by equation 27. Substituting explicit finite-difference approximations for the terms in equation 27, we have

$$(\Delta C_{i,j,k})_{II} = \frac{\Delta t}{\epsilon b_{i,j,k}}\left[C_{i,j,k-1}\left(S\left[\frac{h_{i,j,k}-h_{i,j,k-1}}{\Delta t}\right] + W_{i,j,k} - \epsilon\left[\frac{b_{i,j,k}-b_{i,j,k-1}}{\Delta t}\right]\right) - C'_{i,j,k} W_{i,j,k}\right]. \quad (39)$$

Equations 28, 37, 38, and 39 together provide a solution to equation 24, which in turn allows us to solve equation 20 and complete the definition of the characteristic curves of equation 15.

Because the processes of convective transport, hydrodynamic dispersion, and mixing are occurring continuously and simultaneously, equations 18, 19, and 20 should be solved simultaneously. However, equations 18 and 19 are solved by particle movement based on implicitly computed heads while equation 20 is solved explicitly with respect to concentrations. Because the change in concentration at a source node due to mixing is proportional to the difference in concentration between the node and the source fluid (see eq 27), the accuracy of estimating the concentration at the node during a time increment will clearly affect the computed change. Similarly, because the change in concentration due to dispersion is proportional to the concentration gradient at a point, the accuracy of estimating the concentration gradient will clearly affect the accuracy of the numerical results. As the position of a front or breakthrough curve advances with time, say from the $k-1$ to k time level, the concentration gradient at any fixed reference point and the concentration differences at sources are continuosly changing. The consequent limitations imposed by estimating nodal concentrations in a strict explicit manner can be minimized by using a two-step explicit procedure in which equation 24 is solved at each node by giving equal weight to concentration gradients computed from the concentrations at the previous time level $(k-1)$ and to concentration gradients computed from concentrations at time level (k^*), which represents the convected position of the front at the new time level (k) prior to adjustments of concentration for dispersion and mixing. Figure 3 illustrates the sequence of calculations to solve equations 18–20 over a given time increment. First the concentration gradients at the previous time level $(k-1)$ are determined at each node. Then the front is convected to a new position for time level k^* based on the velocity of flow and length of the time increment. Next the concentration gradients at each node are recomputed for the new position of the front. The concentration distribution for the new frontal position is then adjusted at each node in two steps: first based on concentration gradients at $k-1$ and second based on concentration gradients at k^*.

The finite-difference approximation to equation 24 may thus be expressed as

$$\Delta C_{i,j,k} = \frac{0.5\,\Delta t}{b}\left[\frac{\partial}{\partial x_i}\left(bD_{ij}\frac{\partial C_{(k-1)}}{\partial x_j}\right) + \frac{C_{(k-1)}\left(S\frac{\partial h}{\partial t} + W - \epsilon\frac{\partial b}{\partial t}\right) - C'W}{\epsilon}\right] + \frac{0.5\,\Delta t}{b}\left[\frac{\partial}{\partial x_i}\left(bD_{ij}\frac{\partial C_{(k^*)}}{\partial x_j}\right) + \frac{C_{(k^*)}\left(S\frac{\partial h}{\partial t} + W - \epsilon\frac{\partial b}{\partial t}\right) - C'W}{\epsilon}\right] \quad (40)$$

in which the appropriate finite-difference approximations for the terms within brackets are indicated by equations 37, 38, and 39.

The new nodal concentrations at the end of time increment k are computed as

$$C_{i,j,k} = C_{i,j,k^*} + \Delta C_{i,j,k} \quad (41)$$

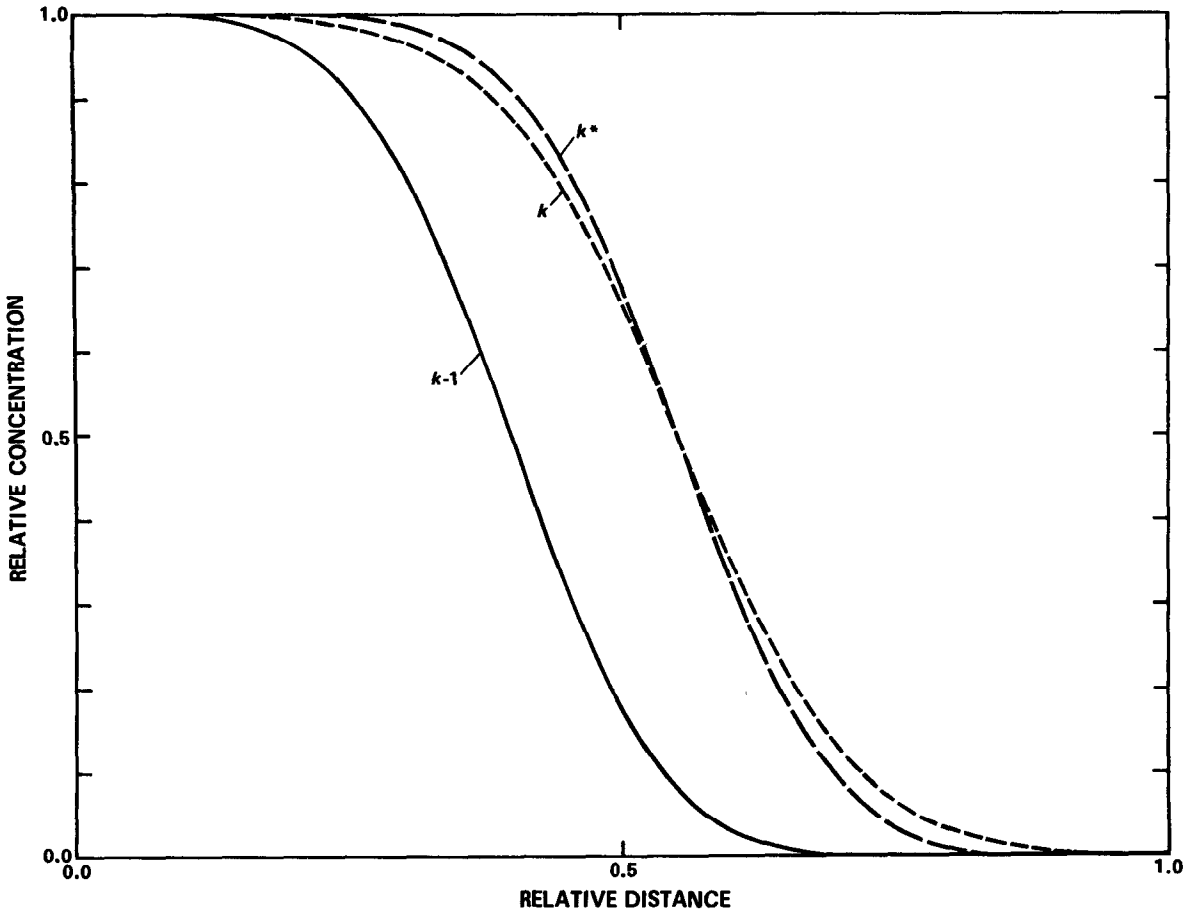

Figure 3.—Representative change in breakthrough curve from time level $k-1$ to k. Note that concentration changes are exaggerated to help illustrate the sequence of calculations.

where $C_{i,j,k*}$ is the average of the concentrations of all points in cell (i,j) after equations 22 and 23 were solved for all points for time step k, and $\Delta C_{i,j,k}$ is the change in concentration caused by hydrodynamic dispersion, sources, and sinks, as calculated in equation 40.

Because the concentrations of points in a cell vary about the concentration of the node, the change in concentration computed at a node using equation 40 cannot be applied directly in all cases to the concentrations of the points. If the change in concentration at the node ($\Delta C_{i,j,k}$) is positive, the increase is simply added to the point concentrations. But if the concentration change is negative, it is applied to points in that cell as a percentage decrease in concentration at each point that is equal to the percentage decrease at the node. This technique preserves a mass balance within each cell, but when a decrease in concentration is computed for a node, it will also prevent a possible but erroneous computation of negative concentrations at those points that had a concentration less than that at the node.

Stability criteria

The explicit numerical solution of the solute-transport equation has a number of stability criteria associated with it. These may require that the time step used to solve the flow equation be subdivided into a number of smaller time increments to accurately solve the solute-transport equation.

First, Reddell and Sunada (1970, p. 62) show that for an explicit finite-difference solution of equation 26 to be stable,

$$\frac{D_{xx}\,\Delta t}{(\Delta x)^2}+\frac{D_{yy}\,\Delta t}{(\Delta y)^2}\leq\frac{1}{2}. \qquad (42)$$

Solving equation 42 for Δt, we see that

$$\Delta t\leq \underset{(\text{over grid})}{\text{Min}}\left[\frac{0.5}{\frac{D_{xx}}{(\Delta x)^2}+\frac{D_{yy}}{(\Delta y)^2}}\right]. \qquad (43)$$

Because the solution to equation 26 is actually written as a set of N equations for N nodes, the maximum permissible time increment is the smallest Δt computed for any individual node in the entire grid. The smallest Δt will then occur at the node having the largest value of

$$\frac{D_{xx}}{(\Delta x)^2}+\frac{D_{yy}}{(\Delta y)^2}.$$

Next consider the effects of mixing ground water of one concentration with injected or recharged water of a different concentration, as represented by the source terms in equation 39. The change in concentration in a source node cannot exceed the difference between the source concentration ($C'_{i,j}$) and the concentration in the aquifer ($C_{i,j}$), and the maximum possible change occurs when a source completely flushes out the volume of water in an aquifer cell at the start of a time step. Therefore

$$\Delta C_{i,j,k}\leq C_{i,j,k-1}-C'_{i,j,k}. \qquad (44)$$

After rearranging terms in equation 44, we have

$$\frac{\Delta C_{i,j,k}}{(C_{i,j,k-1}-C'_{i,j,k})}\leq 1.0. \qquad (45)$$

We may isolate the effects of mixing represented in equation 39 by assuming steady-state flow in which $\partial h/\partial t=0$ and $\partial b/\partial t=0$. Then we can rewrite equation 39 as

$$(\Delta C_{i,j,k})_{II}=\frac{\Delta t\,W_{i,j,k}\,(C_{i,j,k-1}-C'_{i,j,k})}{\epsilon b_{i,j,k}}. \qquad (46)$$

After rearranging terms in equation 46, we have

$$\frac{(\Delta C_{i,j,k})_{II}}{(C_{i,j,k-1}-C'_{i,j,k})}=\frac{\Delta t\,W_{i,j,k}}{\epsilon b_{i,j,k}}. \qquad (47)$$

Substituting equation 47 into equation 45 results in

$$\frac{\Delta t\,W_{i,j,k}}{\epsilon b_{i,j,k}}\leq 1.0. \qquad (48)$$

Solving equation 48 for Δt at all nodes yields the following criterion:

$$\Delta t\leq \underset{(\text{over grid})}{\text{Min}}\left[\frac{\epsilon b_{i,j,k}}{W_{i,j,k}}\right]. \qquad (49)$$

A third type of stability check involves the movement of points computed by equations 22 and 23 to simulate convective transport. The distance a particle moves is defined as

$$\delta x=\Delta t\,V_{x[x_{(p,k)},y_{(p,k)}]} \qquad (50)$$

and

$$\delta y=\Delta t\,V_{y[x_{(p,k)},y_{(p,k)}]}. \qquad (51)$$

In effect, this constitutes a linear spatial extrapolation of the position of a particle from one time step to the next. Where streamlines are curvilinear, the extrapolated position of a particle will deviate from the streamline on which it was previously located. This deviation introduces an error into the numerical solution that is proportional to Δt. Thus, it is thought that an accurate computation of concentration changes caused by convective transport requires the maintenance of a relatively uniformly spaced field of marker particles that are moving along relatively smooth and continuous pathlines. Also, if δx is greater than Δx, or δy is greater than Δy, it might be possible for particles to move beyond the boundaries of the grid during one time increment. Thus, for a given velocity field and grid, some restriction must be placed on the size of the time increment to assure that neither δx nor δy exceed some critical distances, called δx^* and δy^*. Therefore

$$\delta x\leq\delta x^* \qquad (52)$$

and

$$\delta y\leq\delta y^*. \qquad (53)$$

These critical distances can be related to the dimensions of the finite-difference grid by

$$\delta x^*=\gamma\Delta x \qquad (54)$$

and

$$\delta y^* = \gamma \Delta y \tag{55}$$

where γ is the fraction of the grid dimensions that particles will be allowed to move ($0 < \gamma \leq 1$).

If we replace the terms in equations 52 and 53 with the corresponding terms from equations 50, 51, 54, and 55, we have

$$\Delta t \, V_{x[x_{(p,k)}, y_{(p,k)}]} \leq \gamma \Delta x \tag{56}$$

and

$$\Delta t \, V_{y[x_{(p,k)}, y_{(p,k)}]} \leq \gamma \Delta y. \tag{57}$$

Because these criteria are governed by the maximum velocities in the system, and since the computed velocity of a tracer particle will always be less than or equal to the maximum velocity computed at a node or cell boundary, we have to check only the latter. Substituting the grid velocities and solving equations 56 and 57 for Δt results in

$$\Delta t \leq \frac{\gamma \Delta x}{(V_x)_{\max}} \tag{58}$$

and

$$\Delta t \leq \frac{\gamma \Delta y}{(V_y)_{\max}}. \tag{59}$$

If the time step used to solve the flow equation exceeds the smallest of the time limits determined by equations 43, 49, 58, or 59, then the time step will be subdivided into the appropriate number of smaller time increments required for solving the solute-transport equation.

Boundary and initial conditions

Obtaining a solution to the equations that describe ground-water flow and solute transport requires the specification of boundary and initial conditions for the domain of the problem. Specifications for solving the flow equation must be compatible with the solution of the solute-transport equation. Several different types of boundary conditions can be incorporated into the solute-transport model. Two general types are incorporated in this model; these are constant-flux and constant-head conditions. These can be used to represent the real boundaries of an aquifer as well as to represent artificial boundaries for the model. The use of the latter can help to minimize data requirements and the areal extent of the modeled part of the aquifer.

A constant-flux boundary can be used to represent aquifer underflow, well withdrawals, or well injection. A finite flux is designated by specifying the flux rate as a well discharge or injection rate for the appropriate nodes. A no-flow boundary is a special case of a constant-flux boundary. The numerical procedure used in this model requires that the area of interest be surrounded by a no-flow boundary. Thus the model will automatically specify the outer rows and columns of the finite-difference grid as no-flow boundaries. No-flow boundaries can also be located elsewhere in the grid to simulate natural limits or barriers to ground-water flow. No-flow boundaries are designated by setting the transmissivity equal to zero at appropriate nodes, thereby precluding the flow of water or dissolved chemicals across the boundaries of the cell containing that node.

A constant-head boundary in the model can represent parts of the aquifer where the head will not change with time, such as recharge boundaries or areas beyond the influence of hydraulic stresses. In this model constant-head boundaries are simulated by adjusting the leakage term (the last term on the right side of equation 11) at the appropriate nodes. This is accomplished by setting the leakance coefficient (K_z/m) to a sufficiently high value (such as 1.0 s^{-1}) to allow the head in the aquifer at a node to be implicitly computed as a value that is essentially equal to the value of H_s, which in this case would be specified as the desired constant-head altitude. The resulting rate of leakage into or out of the designated constant-head cell would equal the flux required to maintain the head in the aquifer at the specified constant-head altitude.

If a constant-flux or constant-head boundary represents a fluid source, then the chemical concentration in the source fluid (C') must also be specified. If the boundary represents a fluid sink, then the concentration of the produced fluid will equal the concen-

tration in the aquifer at the location of the sink.

Because solute transport directly depends upon hydraulic and concentration gradients, the head and concentration in the aquifer at the start of the simulation period must be specified. The initial conditions can be determined from field data and (or) from previous simulations. It is important to note that the simulation results may be sensitive to variations or errors in the initial conditions. In discussing computed heads, Trescott, Pinder, and Larson (1976, p. 30) state:

> If initial conditions are specified so that transient flow is occurring in the system at the start of the simulation, it should be recognized that water levels will change during the simulation, not only in response to the new pumping stress, but also due to the initial conditions. This may or may not be the intent of the user.

Mass balance

Mass balance calculations are performed after specified time increments to help check the numerical accuracy and precision of the solution. The principle of conservation of mass requires that the cumulative sums of mass inflows and outflows (or net flux) must equal the accumulation of mass (or change in mass stored). The difference between the net flux and the mass accumulation is the mass residual (R_m) and is one measure of the numerical accuracy of the solution. Although a small residual does not prove that the numerical solution is accurate, a large error in the mass balance is undesirable and may indicate the presence of a significant error in the numerical solution.

The model uses two methods to estimate the error in the mass balance. Both are based on the magnitude of the mass residual, R_m, which is computed from

$$R_m = \Delta M_s - M_f \qquad (60)$$

where

ΔM_s is the change in mass stored in the aquifer, M; and

M_f is the net mass flux, M.

The two mass terms, ΔM_s and M_f, are evaluated using the following equations:

$$\Delta M_s = \sum_i \sum_j b_{i,j} \epsilon \Delta x \Delta y (C_{i,j,k} - C_{i,j,o}) \qquad (61a)$$

where $C_{i,j,o}$ is the initial concentration at node (i,j), M/L^3; and

$$M_f = \sum_i \sum_j \sum_k W_{i,j,k} \Delta x \Delta y \Delta t_k C'_{i,j,k}. \qquad (61b)$$

The percent error (E) in the mass balance is computed first by comparing the residual with the average of the net flux and net accumulation, as

$$E_1 = \frac{100.0 (M_f - \Delta M_s)}{0.5 (M_f + \Delta M_s)}. \qquad (62)$$

This is a good measure of the accuracy of the numerical solution when the flux and the change in mass stored are relatively large. However, equation 62 does not account for the initial mass of solute in the aquifer. If total fluxes are very small compared to the initial mass of solute in the aquifer, then equation 62 might indicate a relatively large error when the numerical solution is actually quite accurate. Therefore, the error may also be computed a second way by comparing the residual with the initial mass of solute (M_0) present in the aquifer, as

$$E_2 = \frac{100.0 (M_f - \Delta M_s)}{M_0}. \qquad (63)$$

Equation 63 provides a good measure of the accuracy of the numerical solution when fluxes are zero or relatively small. But when M_0 is zero or very small in comparison to ΔM_s, then E_2 becomes meaningless. This problem can be overcome by correcting M_0 in the denominator of equation 63 for the net mass flux, resulting in

$$E_3 = \frac{100.0 (M_f - \Delta M_s)}{M_0 - M_f}. \qquad (64)$$

Note that as M_f becomes very small, equation 64 approaches equation 63, and as M_0 becomes very small, E_3 becomes just a comparison of the residual with the net flux. In the latter case E_3 is a mass balance indicator similar to E_1 in equation 62. Thus, E_3 is considered a more reliable and versatile indicator of numerical accuracy than is E_2. Either one or both of E_1 and E_3 are computed by the model, as appropriate.

Special problems

There are a number of special problems associated with the use of the method of characteristics to solve the solute-transport equation. Some of these problems are associated with the movement and tracking of particles, while other problems are related to the computational transition between the concentrations of particles within a cell and the average concentration at that node. We will next describe the more significant problems and the procedures used to minimize errors that might result from them.

One possible problem is related to no-flow boundaries. Neither water nor dissolved chemicals can be allowed to cross a no-flow boundary. However, under certain conditions it might be possible for the interpolated velocity at the location of a particle near a no-flow boundary to be such that the particle will be convected across the boundary during one time increment. Figure 4 illustrates such a possible situation, which arises from the deviation between the curvilinear flow line and the linearly projected particle path. If a particle is convected across a no-flow boundary, then it is relocated within the aquifer by reflection across the boundary, as also shown in figure 4. This correction thus will tend to relocate the particle closer to the true flow line.

Fluid sources and sinks also require special treatment. Because they tend to represent singularities in the velocity field, the use of a central difference formulation (eq 12) to compute the velocity at a node may indicate zero or very small velocities at the nodes. Therefore, the velocity components at a source or sink node cannot be used for interpolation of the velocity at a point within or adjacent to that cell. To help maintain radial flow to or from a sink or source, respectively, the velocities computed on the boundaries of source or sink cells are assigned to that node. The appropriate boundary velocities are determined on the basis of the quadrant of interest. This can be illustrated by referring again to figure 2. If a point is located in the southeast quadrant of cell (i,j), the x velocity at node (i,j) would

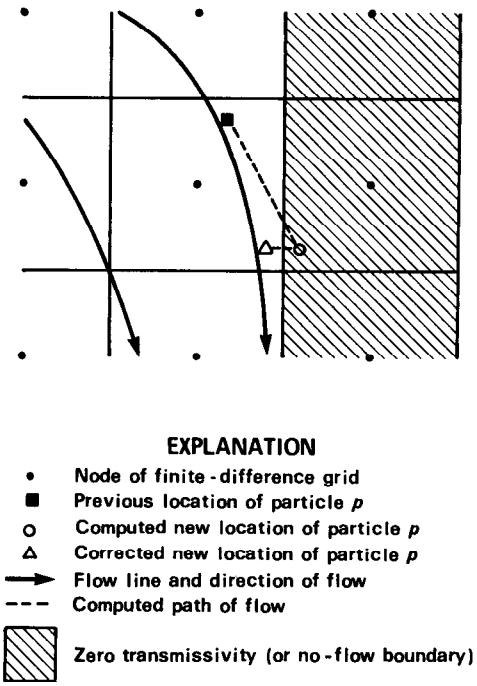

Figure 4.—Possible movement of particles near an impermeable (no-flow) boundary.

be set equal to $V_{x(i+\frac{1}{2},j)}$ and the y velocity to $V_{y(i,j+\frac{1}{2})}$. Corresponding adjustments are made for points in other quadrants, so that the magnitude and direction of velocity at the node are not fixed for a given time increment, but depend on the relative location of the point of interest within the cell. A similar approximation is made when a point of interest is located in a cell adjacent to a source or sink. Thus, if the same point, p, in figure 2 were located in an unstressed cell but the adjacent cell $(i+1,j)$ represented a source or sink, then the y velocity at node $(i+1,j)$ would be approximated by $V_{y(i+1,j+\frac{1}{2})}$ in order to estimate the y velocity at point p. A corresponding approximation for the x velocity at node $(i,j+1)$ would be made using $V_{x(i+\frac{1}{2},j+1)}$ if a source or sink were located at $(i,j+1)$.

The maintenance of a reasonably uniform and continuous spacing of points requires special treatment in areas where sources and sinks dominate the flow field. Points will continually move out of a cell that represents a source, but few or none will move in to re-

place them and thereby maintain a continuous stream of points. Thus, whenever a point that originated in a source cell moves out of that source cell, a new point is introduced into the source cell to replace it. Placement of new points in a source cell is compatible with and analogous to the generation of fluid and solute mass at the source.

The procedure used to replace points in source cells that are adjacent to no-flow boundaries is illustrated in figure 5. Here a steady, uniformly spaced stream of points is maintained by generating a new point at the same relative position in the source cell as the new position in the adjacent cell of the point that left the source cell. As an example, point 7 was convected from cell $(i-1,j)$ to cell (i,j). So the replacement point (22) was placed at a location within cell $(i-1,j)$ that is identical to the new location of point 7 within cell (i,j).

The procedure used to replace points in source cells that lie within the aquifer and not adjacent to a no-flow boundary is illustrated in figure 6. Here a steady, uniformly spaced stream of particles is maintained by generating a new point in the source cell at the original location of the point that left the source cell. When a relatively strong source is imposed on a relatively weak regional flow field, as illustrated in figure 6a, then radial flow will be maintained in the area of the source, and all initial and replacement points will move symmetrically away from node (i,j). For example, after point 7 moves from cell (i,j) to $(i+1, j-1)$, the replacement point (18) is positioned at time k in cell (i,j) at the same location as the initial position of point 7. Although the replacement procedure illustrated earlier by figure 5 would work just as well for the case illustrated in figure 6a, it would not be satisfactory for the situation presented in figure 6b, which illustrates the imposition of a relatively weak source in a relatively strong regional flow field. In this case the velocity distribution within the source cell does not possess radial symmetry, and the velocity within the upgradient part of the source cell is much lower than the velocity within the downgradient part of the source cell. Replacement of points at original locations in source cells, as illustrated in figure 6b, will maintain a steady stream of points leaving the source cell in proportion to the velocity field. However, the use of the procedure illustrated in figure 5 for the case presented in figure 6b would result in the accumulation of

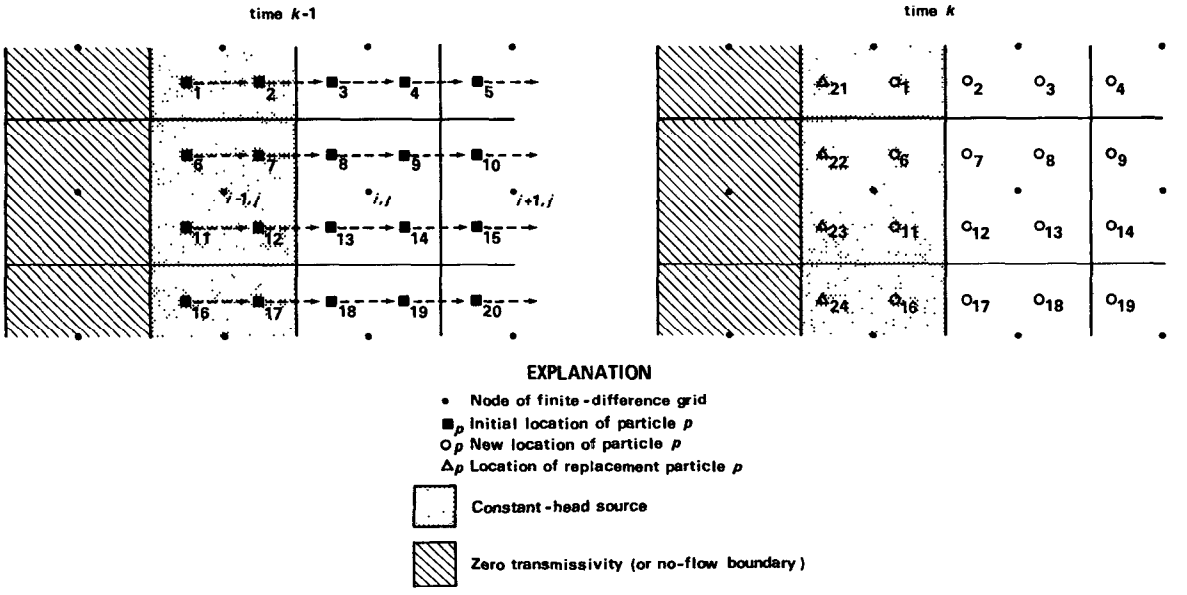

Figure 5.—Replacement of points in source cells adjacent to a no-flow boundary.

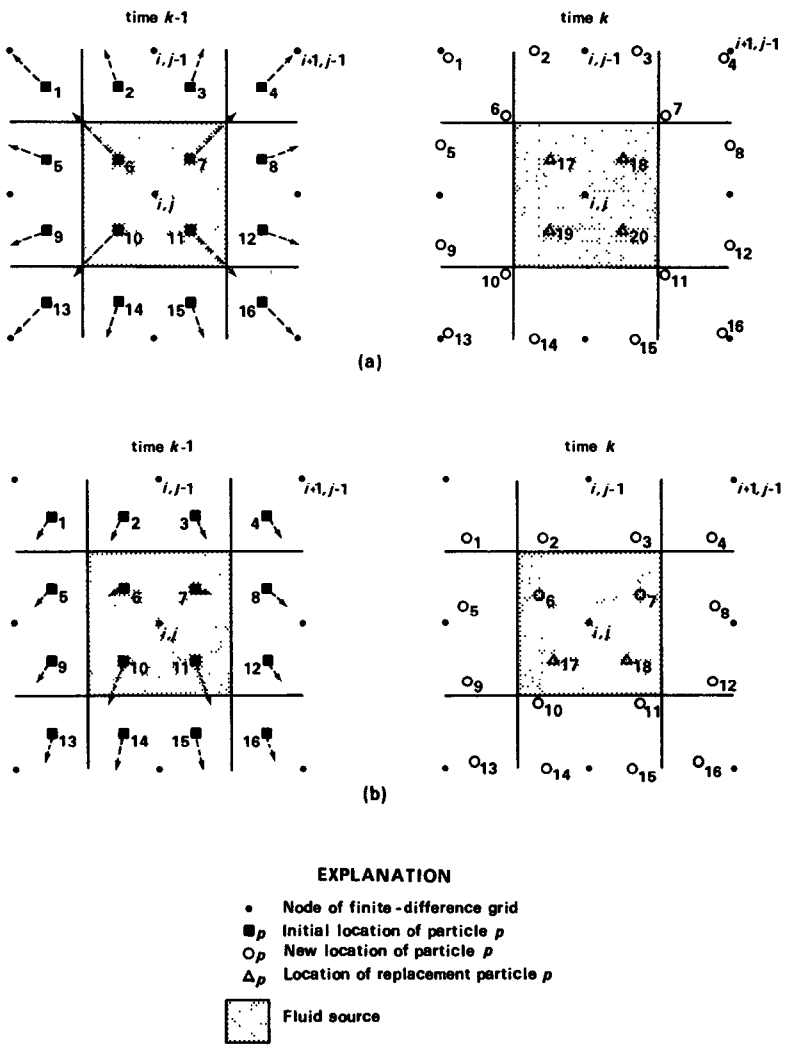

Figure 6.—Replacement of points in source cells not adjacent to a no-flow boundary for negligible regional flow (a) and for relatively strong regional flow (b).

points in the low-velocity area of the source cell (i,j), with few points being replaced into the high-velocity area, where convective transport is the greatest.

Although we normally expect points to be convected out of source cells, figure 6b also demonstrates the possibility that points may sometimes enter a source cell. This can also occur when two or more source cells of different strengths are adjacent to each other. An erroneous multiplication of points might then result if points that did not originate in a particular source cell are replaced when they in turn are convected out of that source cell. Therefore, points leaving a source cell are replaced only if they had originated in that source cell.

Hydraulic sinks also require some special treatment. Points will continually move into a cell representing a strong sink, but few or none will move out. To avoid the resultant crowding and stagnation of tracer points, any point moving into a sink cell is removed from the flow field after the calculations for that time increment have been completed. The numerical removal of points which enter

sink cells is analogous to the withdrawal of fluid and solute mass through the hydraulic sink. The combination of creating new points at sources and destroying old points at sinks will tend to maintain the total number of points in the flow field at a nearly constant value.

Both the flow model and the transport model assume that sources and sinks act over the entire cell area surrounding a source or sink node. Thus, in effect, heads and concentrations computed at source or sink nodes represent average values over the area of the cell. Part of the total concentration change computed at a source node represents mixing between the source water at one concentration and the ground water at a different concentration (eq 39). It can be shown from the relationship between the source concentration ($C'_{i,j,k}$) and the aquifer concentration ($C_{i,j,k-1}$), as indicated by equation 44, that the following constraints generally must be met in a source cell:

$$C_{i,j,k} \leqq C'_{i,j,k} \quad \text{for} \quad C'_{i,j,k} > C_{i,j,k-1} \qquad (65a)$$

and

$$C_{i,j,k} \geqq C'_{i,j,k} \quad \text{for} \quad C'_{i,j,k} < C_{i,j,k-1}. \qquad (65b)$$

If it is assumed that the sources act over the area of the source cell and that there is complete vertical mixing, then these same constraints should also apply to all points within the cell. Because of the possible deviation of the concentrations of individual points within a source cell from the average concentration, the change in concentration computed at a source node ($\Delta C_{i,j,k}$) should not be applied directly to each of the points in the cell. Rather, at the end of each time increment the concentration of each point in a source cell is updated by setting it equal to the final nodal concentration. Although this may introduce a small amount of numerical dispersion by eliminating possible concentration variations within the area of a source cell, it prevents the adjustment of the concentration at any point in the source cell to a value that would violate the constraints indicated by equation 65.

In areas of divergent flow there may be a problem because some cells can become void of points where pathlines become spaced widely apart. This would result in a calculation of zero change in concentration at a node due to convective transport, although the nodal concentration would still be adjusted for changes caused by hydrodynamic dispersion (eq 28). Also, some numerical dispersion is generated at nodes in and adjacent to the cells into which the convective transport of solute was underestimated because of the resulting error in the concentration gradient. This might not cause a serious problem if only a few cells in a large grid became void or if the voiding were transitory (that is, if upgradient points were convected into void cells during later or subsequent time increments). Figure 6a illustrates radial flow, which represents the most severe case of divergent flow. Here it can be seen that when four points per cell are used to simulate convective transport, then in the numerical procedure four of the eight surrounding cells would erroneously not receive any solute by convection from the adjacent source. If eight points per cell were used initially, then at a distance of two rows or columns from the source only 8 of 16 cells would be on pathlines originating in the source cell. So, while increasing the initial number of points per cell would help, it is obvious that for purely radial flow, an impractically large initial number of points per cell would be required to be certain that at least one particle pathline passes from the source through every cell in the grid.

The problem of cells becoming void of particles can be minimized by limiting the number of void cells to a small percentage of the total number of cells that represent the aquifer. If the limit is exceeded, the numerical solution to the solute-transport equation is terminated at the end of that time increment and the "final" concentrations at that time are saved. Next the problem is reinitialized at the time of termination by regenerating the initial particle distribution throughout the grid and assigning the "final" concentrations at the time of termination as new "initial" concentrations for nodes and particles. The solution to the solute-transport

equation is then simply continued in time from this new set of "initial" conditions until the total simulation period has elapsed. This procedure preserves the mass balance within each cell but also introduces a small amount of numerical dispersion by eliminating variations in concentration within individual cells.

To help minimize the amount of numerical dispersion resulting from the regeneration of points, the program also includes an optimization routine that attempts to maintain an approximation of the previous concentration gradient within a cell. The optimization routine aims to meet the following constraints:

$$\frac{\sum_{n=1}^{N_p} C_n^*}{N_p} = C_{i,j} \qquad (66a)$$

$$C_{i,j} \leq C_n^* \leq C_{l,m} \quad \text{for} \quad C_{i,j} \leq C_{l,m} \qquad (66b)$$

and

$$C_{l,m} \leq C_n^* \leq C_{i,j} \quad \text{for} \quad C_{i,j} \geq C_{l,m} \qquad (66c)$$

where

C_n^* is the concentration of the nth point in cell (i,j), M/L^3;

N_p is the total number of points initially placed in a cell; and

$C_{l,m}$ is the concentration at node (l,m), which represents a cell adjacent to (i,j) and on a line that starts at (i,j) and extends through the coordinates of the point (n) of interest, as illustrated in figure 7, M/L^3.

Note that equation 66a simply indicates that a mass balance must be preserved in a cell regardless of the range in variation of point concentrations within the cell. Equations 66b and c indicate that the concentration of any point must lie between $C_{i,j}$ and the concentration at the node adjacent to particle n. The coordinates of the adjacent node would take on values of $l=i$ or $l=i\pm1$ and $m=j$ or $m=j\pm1$. For example, figure 7 shows that for point 2, the coordinates (l,m) would equal $(i,j-1)$, while for point 3, (l,m) would equal $(i+1,j-1)$. The optimization routine is written so that if equations 66a–c cannot be satisfied simultaneously for node (i,j) within two iterations, then to avoid further computational delay all C_n^* are simply set equal to $C_{i,j}$.

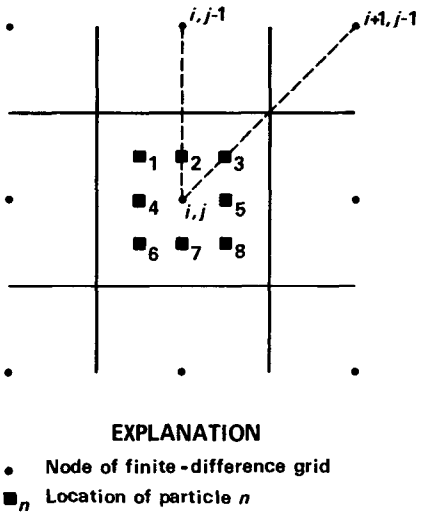

Figure 7.—Relation between possible initial locations of points and indices of adjacent nodes.

Computer Program

The computer program serves as a means of translating the numerical algorithm into machine executable instructions. The purpose of this chapter is to describe the overall structure of the program and to present a detailed description of its key elements, thereby providing a link between the numerical methods and the computer code. We hope that this link will make it easier for the model user to understand and, if necessary, modify the program. The FORTRAN IV source program developed for this model is listed in attachment I and includes almost 2,000 lines. For reference purposes columns 73–80 of each line contain a label that is numbered sequentially within each subroutine. The definition of selected variables used in the program is presented in attachment II; this glossary therefore also serves as a key for relating the program variables

to their corresponding mathematical terms. The computer program is compatible with many scientific computers; it has been successfully run on Honeywell, IBM, DEC, and CDC computers.

General program features

The program is segmented into a main routine and eight subroutines. The name and primary purpose of each segment are listed in Table 1. Each program segment will be described in more detail in later sections of this chapter.

Table 1.—List of subroutines for solute-transport model

Name	Purpose
MAIN	Control execution.
PARLOD	Data input and initialization.
ITERAT	Compute head distribution.
GENPT	Generate or reposition particles.
VELO	Compute hydraulic gradients, velocities, dispersion equation coefficients, and time increment for stable solution to transport equation.
MOVE	Move particles.
CNCON	Compute change in chemical concentrations and compute mass balance for transport model.
OUTPT	Print head distribution and compute mass balance for flow model.
CHMOT	Print concentrations, chemical mass balance, and observation well data.

The major steps in the calculation procedures are summarized in figure 8, which presents a simplified flow chart of the overall structure of the computer program. The flow chart illustrates that the tracer particles may have to be moved more than once to complete a given time step. In other words, the time step used to implicitly solve the flow equation may have to be subdivided into a number of smaller time increments for the explicit solution of the solute-transport equation. The maximum time increments allowable for the explicit calculations are computed automatically by the model. Thus, the model user cannot specify an erroneously large increment or an inefficiently small increment for solving the solute-transport equation. For transient flow problems, some discretion is still required in the specification of the initial time step and of the time-step multiplier, as discussed by Trescott, Pinder, and Larson (1976, p. 38–40).

The general program presented here is written to allow a grid having up to 20 rows and 20 columns. Because the numerical procedure requires that the outer rows and columns represent no-flow boundaries, the aquifer itself is then limited to maximum dimensions of 18 rows and 18 columns. If a problem requires a larger grid, then the appropriate arrays must be redimensioned accordingly. These arrays are contained in COMMON statements PRMK, HEDA, HEDB, CHMA, CHMC, and DIFUS, and in DIMENSION statements on lines C170, G200, H140, and I160.

The program allows the specification of one pumping well per node. The wells can represent injection (recharge) or withdrawal (discharge). If more than one well exists within the area of a cell, then the flux specified for that node should represent the net rate of injection or withdrawal of all wells in that cell. The model assumes that stresses are constant with time during each pumping period (NPMP). But the total number of wells, as well as their locations, flux rates, and source concentrations, may be changed for successive pumping periods. The program also allows the specification of observation wells at as many as five nodes in the grid. For nodes that are designated as observation wells, at the end of the simulation period or after every 50 time increments the model will print a summary table of the head and concentration at the previous time increments.

The program also includes a node identification array (NODEID), which allows certain nodes or zones to be identified by a unique code number. This feature can save much time in the preparation of input data by easily equating each code number with a desired boundary condition, flux, or source concentration.

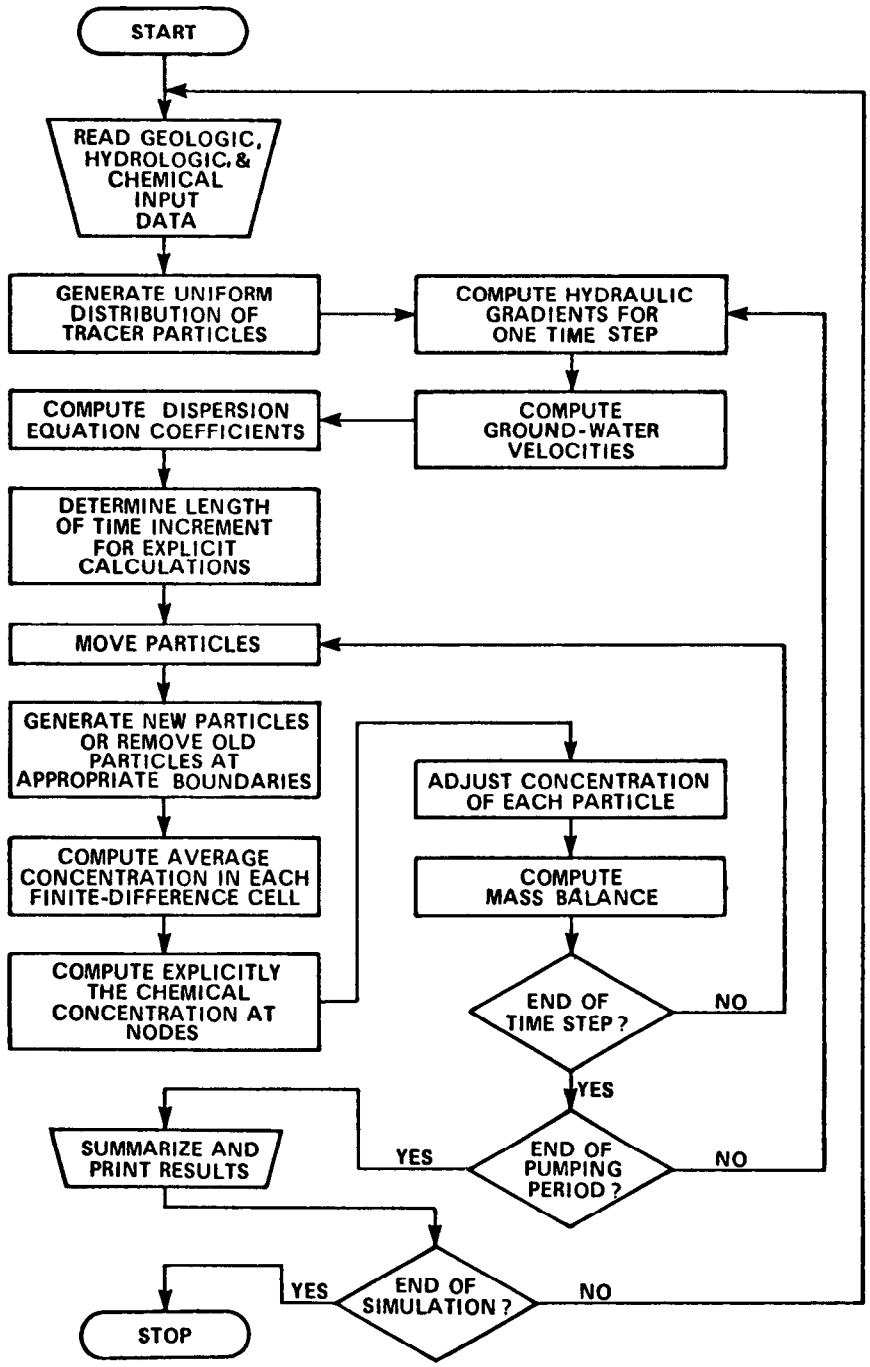

Figure 8.—Simplified flow chart illustrating the major steps in the calculation procedure.

Program segments

MAIN

The primary purpose of the MAIN routine is to control the overall execution sequence of the program. Subroutines for input, execution, and output are called from MAIN and the elapsed time simulated is compared with the desired total simulation period. Also, lines A500–A580 serve to store (or

record) observation well data for transient flow problems.

Subroutine PARLOD

All input data are read through subroutine PARLOD. These data define the properties, boundaries, initial conditions, and stresses for the aquifer, as well as spatial grid and time-step factors. The values of many variables are also initialized here. After the data are read, some preliminary calculations are made, such as (1) determining time increments for the flow model (lines B780–B890), (2) computing the harmonic mean transmissivities in the x and y directions (B1670–B1800), (3) adjusting transmissivity for anisotropy (B1810–B1820), (4) computing iteration parameters (B1840–B1910 and B2880–B2980), and (5) checking for possible inconsistencies among the input data (B3140–B3290). A printout is also provided of all input data so that the data may be rechecked and each run identified.

Subroutine ITERAT

This subroutine solves a finite-difference approximation of the flow equation (eq 11) using an iterative ADI procedure. The matrix generated by the finite-difference approximation is solved using the Thomas algorithm, as described by von Rosenberg (1964, p. 113). Row calculations are made in lines C270–C610, and column calculations are made in lines C630–C970. The calculations are assumed to have converged on a solution if the maximum difference at all nodes between heads computed along rows and heads computed along columns is less than the specified tolerance. Convergence is checked on lines C940–C950. Note that here (for example, lines C380, C700, C930, and C1150) and in other subroutines the thickness array (THCK) is used to check whether a node is in the aquifer.

It should also be noted here that the flow model, as written, assumes that the transmissivity of the aquifer is independent of the head (or saturated thickness) and remains constant with time. If this assumption is not appropriate to the particular aquifer system being modeled, then the solution algorithm presented in this subroutine should be modified accordingly. For example, flow models published by Prickett and Lonnquist (1971, p. 43–45) and Trescott, Pinder, and Larson (1976) include such a modification.

All parameters involved in the calculation of heads are defined as double precision variables and all calculations involving these parameters are performed in double precision. The number of double precision variables and operations can be reduced significantly if the program is to be executed on a high-precision scientific computer, thereby improving the efficiency of the model by reducing computer storage requirements and execution time.

The iterative ADI procedure used to solve the finite-difference equations is not necessarily the best possible solution technique for all problems. For example, it may be difficult to obtain a solution using the iterative ADI procedure for cases of steady-state flow when internal nodes in the grid have zero transmissivity and for cases in which the transmissivity is highly anisotropic. In such cases, a strongly implicit procedure, such as the one documented by Trescott, Pinder, and Larson (1976), should be substituted for the solution algorithm contained in subroutine ITERAT.

Subroutine GENPT

The primary purpose of subroutine GENPT is to generate a uniform initial distribution of tracer particles throughout the finite-difference grid. This is done either at the start of a simulation period or at an intermediate time when too many cells have become void of particles. In the latter case, the program attempts to preserve an approximation of the previous concentration gradient within each cell (lines D1420–D2040).

The placement of particles is accomplished in lines D510–D1410. The program allows the placement of either four, five, eight, or nine particles per cell. Of course each option will result in a slightly different geometry

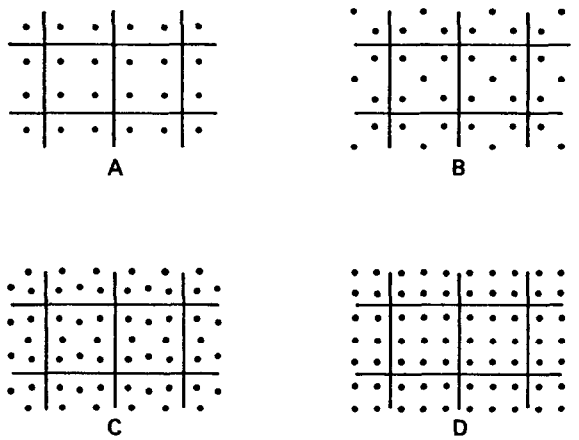

Figure 9.—Parts of finite-difference grids showing the initial geometry of particle distribution for the specification of four (*A*), five (*B*), eight (*C*), and nine (*D*) particles per cell.

and density of points, as illustrated by figure 9. The most regular or uniform patterns are produced when four or nine particles per cell are specified. If a different number of particles per cell or a different placement geometry are desired, this subroutine could be modified accordingly.

As particles are moved or convected through the grid during the calculation procedure, there is a need to remove particles at fluid sinks and create particles at fluid sources. A buffer array (called LIMBO) is created on lines D430–D480 that contains particles that can be added later to the grid at sources and that also contains space to store particles removed at sinks or discharge boundaries.

Subroutine VELO

Subroutine VELO accomplishes three objectives. First, it computes the flow velocities at nodes and on cell boundaries by solving equations having the form of equations 12 and 13. The velocities are computed on lines E420–E680. Second, the dispersion equation coefficients are calculated. These coefficients represent terms factored out of equations 37 and 38, as follows:

$$\text{DISP(IX,IY,1)} = (bD_{xx})_{[i+\frac{1}{2},j]}/(\Delta x)^2 \quad (67a)$$

$$\text{DISP(IX,IY,2)} = (bD_{yy})_{[i,j+\frac{1}{2}]}/(\Delta y)^2 \quad (67b)$$

$$\text{DISP(IX,IY,3)} = (bD_{xy})_{[i+\frac{1}{2},j]}/4\Delta x\Delta y \quad (67c)$$

$$\text{DISP(IX,IY,4)} = (bD_{yx})_{[i,j+\frac{1}{2}]}/4\Delta x\Delta y. \quad (67d)$$

Note that each dispersion coefficient (D_{xx}, D_{yy}, D_{xy}, D_{yx}) is computed on cell boundaries using the relationships expressed in equations 8–10. Therefore, the equation coefficients computed by equation 67 are stored as forward values from the indicated node in the DISP array. Third, this subroutine computes (on lines E1050–E1240 and E1800–E1930) the minimum number of particle moves (NMOV) required to solve the transport equation for the given time step so that the maximum time increment for the transport equation solution will not exceed any of the criteria indicated by equations 43, 49, 58, and 59.

Subroutine MOVE

Although this subroutine has only one main function, which is to move the tracer particles in accordance with equations 22 and 23, it is the longest and perhaps the most complex segment of the program. The complexities are mainly introduced by the treatment of particles at the various types of boundary conditions. To help illustrate the calculation procedure followed within subroutine MOVE, a flow chart is presented in figure 10. The numbers in the flow chart indicate the corresponding lines in subroutine MOVE where the indicated operation is executed.

If a node represents a fluid source or sink, then particles must be respectively created or destroyed in these cells. If the value of pumpage (REC) at a node does not equal zero, then the node is assumed to represent either a fluid source (for REC$<$0) or a fluid sink (for REC$>$0). Recharge or discharge can also be represented by the RECH array. But it is assumed that this type of flux is sufficiently diffuse so that it does not induce areas or points of strongly divergent or convergent flow and therefore particles need not be created or destroyed at these nodes. Note that here and in other subroutines the presence of a constant-head boundary is tested by checking the value of leakance (VPRM)

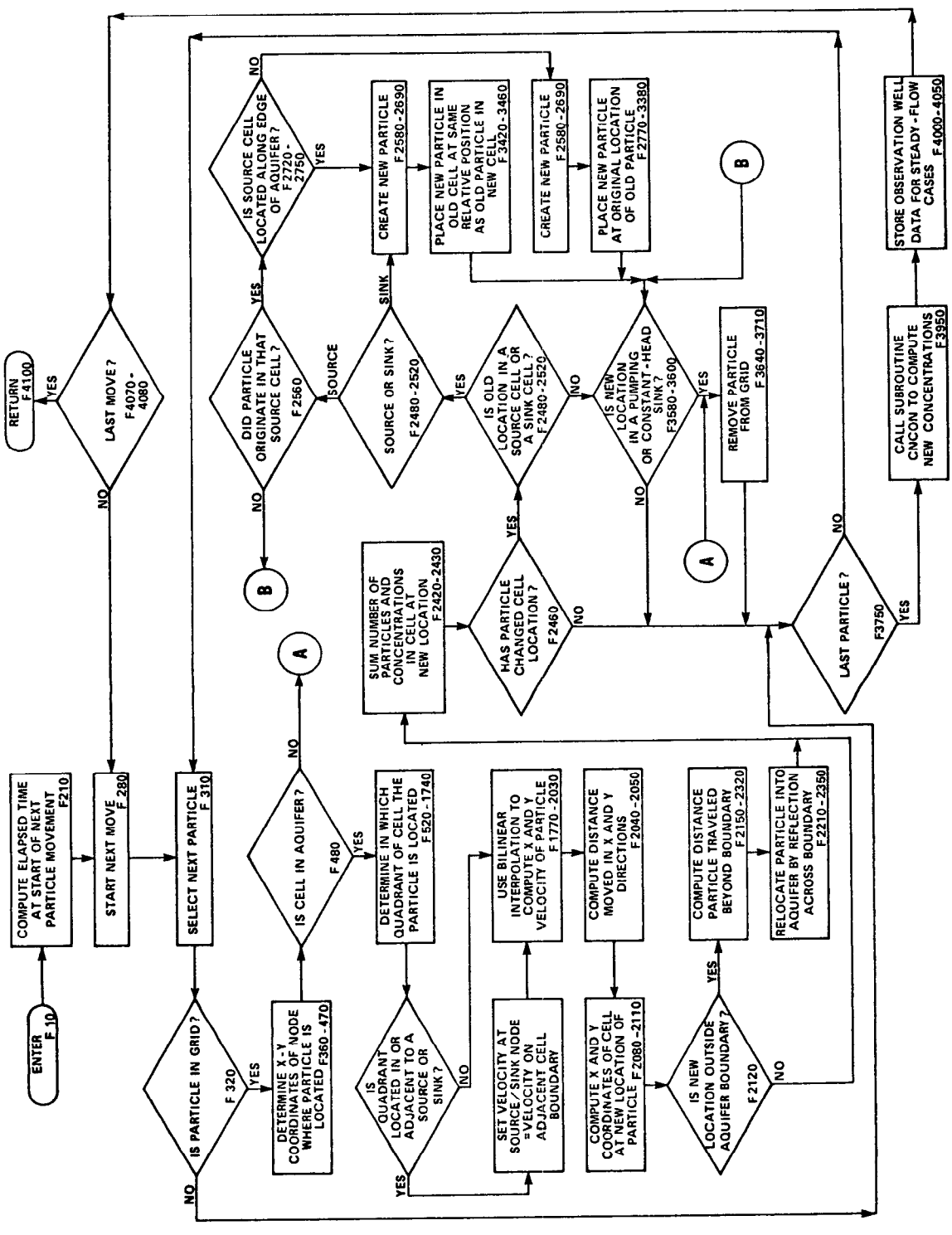

Figure 10.—Generalized flow chart of subroutine MOVE. Numbers indicate line numbers where the operation is executed.

at each node. If VPRM exceeds 0.09, it is assumed that the node represents a constant-head boundary condition and is treated as a fluid source or sink accordingly. At a constant-head node the difference in head between the aquifer and the source bed is used to determine whether the node represents a fluid source or sink (for example, lines F2500–F2520).

Subroutine CNCON

This subroutine computes the change in concentration at each node and at each particle for the given time increment. Equation 39, which denotes the change in concentration resulting from sources, divergence of velocity, and changes in saturated thickness, is solved on lines G350–G610. On the G520 the value of the storage coefficient is checked to determine whether the aquifer is confined or unconfined. It assumes that if $S<0.005$, then the aquifer is confined and $\partial b/\partial t=0$. If $S\geqq 0.005$, the model assumes that $\partial b/\partial t = \partial h/\partial t$. If this criterion is not appropriate to a particular aquifer system, then line G520 should be modified accordingly. The change in concentration caused by hydrodynamic dispersion is computed on lines G640–G770 as indicated by equations 37 and 38.

The nodal changes in concentration caused by convective transport are computed on lines G850–G940. The number of cells that are void of particles at the new time level are also counted in this set of statements on lines G880–G910, and then compared with the critical number of void cells (NZCRIT) to determine if particles should be regenerated at initial positions before the next time level is started (lines G960–G1020).

The new (time level k) concentrations at nodes are computed on the basis of the previous concentration at time $k-1$ and the change during $k-1$ to k. The adjustment at nodes is accomplished on lines G1060–G1180, while the concentration of particles is adjusted on lines G1210–G1360.

A mass balance for the solute is next computed (lines G1400–G1730) at the end of each time increment. In computing the mass of solute withdrawn or leaking out of the aquifer at fluid sinks, the concentration at the sink node is assumed to equal the nodal concentration computed at time level $k-1$.

Subroutine OUTPT

This subroutine prints the results of the flow model calculations. When invoked, the subroutine prints (1) the new hydraulic head matrix (lines H190–H260), (2) a numeric map of head values (H300–H390), and (3) a drawdown map (H510–H710). This subroutine also computes a mass balance for the flow model and estimates its accuracy (H420–H820). A mass balance is performed both for cumulative volumes since the initial time and for flow rates during the present time step. The mass balance results are printed on lines H840–H930.

Subroutine CHMOT

This subroutine prints (1) maps of concentration (lines I250–I380), (2) change in concentration from initial conditions (I440–I580), and (3) the results of the cumulative mass balance for the solute (I670–I860). The accuracy of the chemical mass balance is estimated on lines I610–I660 using equations 62 and 64. The former is not computed if there was no change in the total mass of solute stored in the aquifer. The latter is not computed if the initial concentrations were zero everywhere. Lines I890–I1140 serve to print the head and concentration data recorded at observation wells. These data are recorded after each time step for a transient flow problem and after each particle movement for a steady-state flow problem. The data are printed after every 50 time increments and at the end of the simulation period.

Evaluation of Model

Comparison with analytical solutions

The accuracy of the numerical solution to the solute-transport equation can be evalu-